Research Article | Vol. 33, No. 12 / 16 Jun 2025 / Optics Express 25159
Optics EXPRESS

Nitrogen-vacancy color centers in nanodiamonds as reference single-photon emitters

NIKESH PATEL,[1] BENYAM DEJEN,[2] STEPHEN CHURCH,[1,*] PHILIP DOLAN,[2,3] AND PATRICK PARKINSON[1]

[1]Department of Physics & Astronomy and the Photon Science Institute, University of Manchester, Oxford Road, Manchester M13 9PL, United Kingdom
[2]National Physical Laboratory, Hampton Road, Teddington, Middlesex TW11 0LW, United Kingdom
[3]Current address: Nu Quantum, Broers Building, 21 JJ Thomson Avenue, Cambridge CB3 0FA, United Kingdom
*stephen.church@manchester.ac.uk

Abstract: Quantitative and reproducible optical characterization of single quantum emitters is crucial for quantum photonic materials research, yet accounting for measurement conditions remains challenging due to a lack of an established reference standard. We propose nanodiamonds containing single nitrogen vacancy (NV^-) color centers as reliable, stable, and robust reference sources of single-photon emission. We select 4 potential reference emitter candidates from a study of thousands of NV^-centers. Candidates were remeasured at a second laboratory, correlating optical pump power and NV^-center emission intensity at saturation in addition to corresponding $g^{(2)}(0)$ values. A reference nanodiamond is demonstrated to account for experimental conditions, with reproducible and reliable single-photon emission, as a model for a new, to our knowledge, single-photon emitter reference standard.

1. Introduction

Single-photon emitters (SPEs) will play a ubiquitous role in quantum technologies 2.0, motivated by growing interest in applications such as quantum sensing [1], computing [2,3] and communication [4]. However, realization of triggerable (also referred to as "on-demand" or "deterministic") SPEs for quantum photonic technologies, such as quantum key distribution [5], qubit transmission nodes [6] or quantum logic gates [7] remains challenging. Potential SPEs include defects in bulk crystals [8–10], self-assembled quantum dots [4], colloidal quantum dots [11,12] or quantum dot-in-nanowire systems [13–17]. CQDs have emerged as a promising SPEs due to their exceptional quantum yield [18], along with perovskite quantum dots with high single-photon purity [19], local strain-activated SPEs in transition metal dichalcogenides (TMDs) [20,21] and hexagonal boron nitride (hBN) [22]. These materials can be further modified by adding optical reflectors [23], surface passivation or hosting quantum dots in photonic cavities [24,25] and metasurfaces [26] to enhance the spectral density of emission. However, accurate and reproducible comparison of novel single-photon emitting materials, which often incorporate anisotropic photonic enhancements remains problematic [27] due to the lack of a reference with a known single-photon emission rate. A suitable reference must allow quantitative comparison between multi-photon emission probability as measured by the second-order degree of coherence [28], $g^{(2)}(t)$, single-photon emission rate, and saturation pumping rate. The emission rates of SPEs are limited by their state emission lifetime, and typically exhibit saturation with increased pump intensity. This is observed as a sub-linear relationship between illumination intensity

#564082 https://doi.org/10.1364/OE.564082
Journal © 2025 Received 2 Apr 2025; revised 17 May 2025; accepted 18 May 2025; published 4 Jun 2025

Optics EXPRESS

and single-photon emission rate [29]. Critically, this relationship can be exploited to excite a system at the same rate using different experimental apparatus. This is achieved by setting the pump power to a fixed rate below saturation, which allows reproducible measurements under fixed internal excitation conditions, enabling quantitative comparison of single-photon emitting materials characterized with different experimental approaches.

Nanodiamonds (NDs) are an ideal single-photon emitter (SPE) [25,30] when they contain a single nitrogen-vacancy (NV^-) color center [31], known to emit single photons on demand [32–35]. They have beneficial SPE characteristics due to stability against photobleaching [35], ease of fabrication [36,37], and room-temperature emission [24,35,38]. NDs are preferred over bulk diamond as the size constraint reduces the probability of hosting multiple NV^- defects, and they can have higher single-photon emission rates due to Purcell enhancement [39,40]. It has been shown that removal of graphite residues [41], contaminants and surface defects can improve performance [42]. Furthermore, NDs are portable as they can be deposited on many substrates, and the charge-conversion process is unaffected by temperature between 20 and 75 °C [43]. Previous studies have explored their use as reference emitters to calibrate single-photon detectors [44,45] and for a comparison of $g^{(2)}(0)$ measurements [46]. Here, we extend these approaches by registering single NV^- defects and demonstrating their use as a portable reference standard.

The NV^- color center is a substitutional nitrogen point defect coupled to an adjacent vacancy site [25,30,47] in the diamond lattice. The nitrogen-vacancy center is stable due to the exceptional chemical and mechanical stability of the diamond lattice [48]. Diffusion of the defect towards the surface occurs on a timescale of centuries [49]. The emission from fluorescent nanodiamonds (FNDs), used in this work, are photostable [50], showing no photobleaching or fluorescent intermittency – even for single NV centers [51].

The fluorescent intensities of milled FNDs are bulk-dependent, and their emission is unaffected by surface properties or environment [50]. However, for detonation nanodiamonds, surface termination species can affect the emission properties, where carboxylated nanodiamonds can reduce the emission by up to 100x compared to other species [52]. For this reason, we preferably use milled FNDs.

Two fluorescent charge states exist [53], NV^0 and NV^-, where the latter is optically active with a lifetime between 9-25 ns [54,55]. Under 532 nm optical pumping, a common wavelength for single-photon experimentation in the visible range, the NV center can be ionized into either state (70% NV^- and 30% NV^0) [56,57], however preferentially favors NV^- at longer excitation wavelengths [55]. NV^- emits with a zero-phonon line (ZPL) at 637 nm, extending up to 800 nm via phonon sidebands, whereas NV^0 emits with a ZPL at 575 nm. The preferred state to use as an SPE is NV^- as it has a significantly shorter lifetime compared to NV^0 [58] and a higher count rate. Even without spectrally filtering the NV^0 emission, the majority of emission originates from NV^-. NV^- centers are known to exhibit emission saturation [29,31], limited by the lifetime of the excited state.

We validate the use of NV^- color centers as single-photon emitter reference standards by measuring the $g^{(2)}(0)$ value, pumping power and count rates at saturation using two systems with different experimental apparatus at room temperature. In this work, 1053 objects were initially examined at the first laboratory (NPL) using a high-throughput quasi-confocal Hanbury Brown and Twiss [59] (HBT) interferometer. This was filtered to 253, according to an intensity threshold which varied depending on the background. This left 111 potential SPE NV^- centers with $g^{(2)}(0) < 0.5$. A subset of 6 NV^- candidate centers, labelled as #A-#F in the text, from the 111 were selected, due to their favourable signal-to-noise ratio (SNR) and a detailed description of the screening process is given (see Supplement 1). These represent 5.41% of the total identified SPEs. These 6 candidates were re-examined at a second laboratory, the University of Manchester (UoM), to check whether their properties were recoverable and 4 of the 6 were verified to contain a single emitter. All parameters were measured at both laboratories and remeasured at UoM to

Optics EXPRESS

assess stability. Measurements were focused on one candidate, which showed repeatability with a 3% standard deviation in count rate at saturation from the measurements obtained in Table 1. Repeatability is a critical aspect for the NV^- centers to serve as a dependable reference, and when coupled with the robust qualities of NV^- centers hosted in NDs, we show these SPEs can be used as an efficacious benchmark for single-photon experimentation.

Table 1. $g^{(2)}(0)$, I_{80}, I_{sat}, P_{sat} and k_∞ values upon repeated measurement of ND #B at UoM (UoM_{1-3}) with reference values measured at NPL (NPL_1). The errors represent a fitting $\pm 1\ \sigma$ standard deviation

Repeat	$g^{(2)}(0)$	I_{80} (kcps)	I_{sat} (kcps)	P_{sat} (μW)	k_∞ (kcps)
NPL_1	0.32(3)	43(4)	47(2)	390(60)	94(5)
UoM_1	0.33(1)	23.4(6)	26.0(5)	43(2)	52(1)
UoM_2	0.20(1)	22.5(6)	25.1(5)	60(2)	50(1)
UoM_3	0.31(1)	24.4(8)	26.6(8)	89(5)	53(2)

2. Methods

2.1. Spincoating nanodiamonds

A silicon substrate was prepared for lithography by cleaning in acetone, isopropyl alcohol and then dried with nitrogen. The silicon was treated in O_2 plasma for 6 minutes prior to photoresist deposition. A photoresist (AZ 5214E, Merck Performance Materials GmbH) was spin-coated at 4000 rpm for 60 s and baked at 110 $^c ircC$ for 2 minutes, forming a 285 nm thick SiO_2 surface layer. A pattern was applied by optical grid mark lithography using a Microtech LW-405B+ using a ring focussed laser producing an energy density (fluence) of 262 mJ cm^{-2}. The exposed substrate was developed in undiluted AZ 726 MIF for 40 s and sonicated in acetone to remove organic residue. The substrate was ozone cleaned to create a hydrophilic surface. FND Biotech brFND-70/50/35/10 1 mg/ml NDs were diluted in deionised water, sonicated, and then dropped onto the patterned substrate until complete coverage and allowed to settle for 60 s. The sample was spincast at 1000 rpm to eject excess material, leaving an approximately 0.03 μm^{-2} isotropic distribution of NDs by analysis of a microscope image (see Supplement 1).

2.2. High-throughput NV^- center identification

The initial search for candidate single emitting NV^- centers at NPL used a high-throughput confocal microscopy system (see Supplement 1) with an HBT collection path containing two single-photon avalanche photodiodes (SPADs) and a PicoQuant PicoHarp 300 time-correlated single-photon counting (TCSPC) module.

A 532 nm continuous wave (CW) laser was directed through a 60× magnification, 0.90 numerical aperture (NA) objective lens by a 550 nm cut-on dichroic mirror, providing a diffraction limited Gaussian spot. The beam was raster-scanned across the sample surface, placed on a platform, in 200 nm steps by using a fast-steering mirror. The NV^- emission was additionally filtered by a 550 nm long-pass filter before being focused by a 10× magnification, 0.26 NA objective into a single-mode patch cable connected to one input fibre of a 50 μm core multi-mode 2×2 fiber beam splitter whose output fibers were each attached to an Excelitas SPCM-AQR-14-FC SPAD. The signals from the SPADs were sent to a PicoHarp 300 TCSPC module operating in time-tagged time-resolved (TTTR) mode. The count rate maps were expressed in counts per second (cps), with bright spots that correspond to emissive NV^- centers. Several 50 μm × 50 μm areas were measured, containing hundreds of NV^- centers per scan. A count rate threshold filtered which NV^- centers to investigate further, in combination with an object finding algorithm (see Supplement 1). A background count rate was recorded before proceeding with

Optics EXPRESS

power dependence measurements on each identified object and its photon stream was acquired for 600 s in TTTR mode at 80% of the pump power saturation point. Six potential single emitting NV^- centers were selected from a pool of 111 potential emitters with $g^{(2)}(0) < 0.5$ and root-mean square error (RMSE) < 0.15 in the regions $|t|>1$ μs. The region $|t|>1$ μs was chosen to evaluate the RMSE as it is sufficiently longer than the NV^- lifetime (12 ns) and other longer-lived states (< 500 ns), therefore corresponding only to background noise within the system.

2.3. Candidate NV^- center validation

The candidate NV^- centers were remeasured at UoM (see Supplement 1) using a 532 nm CW diode-pumped solid state laser which passed through a 532 nm laser line filter. The sample was mounted on a PhysikInstrumente V-738 high-precision XY motor-controlled stage. The laser was focused on the sample by a 100× magnification, 0.85 NA objective lens with an elliptical beam profile (d_{min} = 560 nm, d_{maj} = 740 nm). The emission passed through a 550 nm dichroic mirror, a 550 nm longpass filter and two 532 nm Raman notch filters. The filtered emission was focused by an f = 40 mm lens on to a 50 μm multimode 1×2 fiber beam splitter, attached to two ID Quantique ID100 SPADs. The SPADs were connected to a PicoQuant HydraHarp 400 TCSPC module. Due to the lower light collection efficiency compared to NPL, TTTR data for each candidate ND was acquired for 3600 s at 80% of the pump power saturation point. In some cases, this resulted in a SNR that was insufficient for generating $g^{(2)}(t)$ signals - when this occurred, pumping was performed at a higher power, set to 0.1 mW.

3. Results and discussion

A total of 1053 objects were initially identified at NPL, a subset of this is shown in Fig. 1(a). The 1053 objects were filtered to 253 (24.0%) by rejecting objects that emit below a minimum count rate threshold (see Supplement 1). Count rate, I, and pump power saturation, P_{sat}, were measured as a function of pump power, P, modelled using:

$$I(P) = \frac{k_\infty P}{P + P_{sat}} + cP, \tag{1}$$

where P is the incident power measured at the sample surface, k_∞ is defined as the maximum observable count rate at infinite pump power [60], P_{sat} is the power at half of the maximum observable count rate and c is an experimental parameter accounting for background photon flux as a function of pump power [31]. The NV^- count rate at pump power saturation is $I(P_{sat})=\frac{k_\infty}{2}$. The first term in Eq. (1) corresponds to emission from the NV^- center and the second term is proportional to the laser pump signal. Fig. 1(b) shows by setting pump power to 80% of P_{sat}, we ensure that the NV^- center is excited at the same rate at UoM as at NPL. NV^- center #B can be used as a reference single-photon emitter associated with a count rate denoted as $I_{80} = I(0.8P_{sat})$. This condition allows quantitative comparison between the NV^- centers measured at UoM and NPL, therefore $g^{(2)}(t)$ data was acquired at this power. The $g^{(2)}(t)$ signals, in Fig. 1(c), were fit by a three-level model [53] using Eq. (2). The first exponential term accounts for the anti-bunching from the NV^- centers, with a bunching contribution in the second exponential:

$$g^{(2)}(t) = 1 - a\left[(b)\exp\left(\frac{-|t-t_0|}{\tau_{NV}}\right) + (1-b)\exp\left(\frac{-|t-t_0|}{\tau_L}\right)\right] \tag{2}$$

where $1 - a = g^{(2)}(0)$, b is a weighting factor between the two exponent terms, τ_{NV} is the anti-bunching lifetime and τ_L represents bunching from longer-lived contributions at finite delay times where $|t|>>\tau_{NV}$. Contributions to τ_L come from shelving to a metastable state [30,35,53,55,61] and charge state switching [62–58] between the NV^0 and NV^- states. t_0 accounts for an arbitrary delay time shift in the $g^{(2)}(0)$ dip, due to a relative time delay between the SPADs, resulting in an offset between photon arrival times at each channel.

Optics EXPRESS

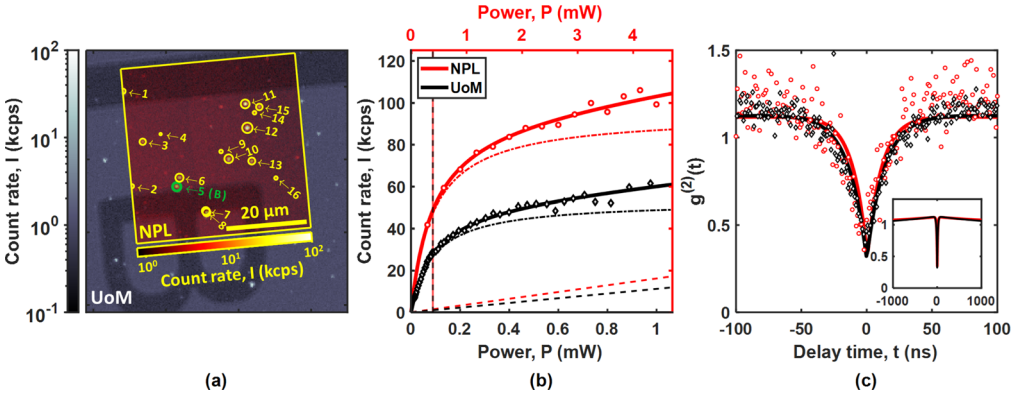

Fig. 1. a) Overlayed count rate maps of a region measured for NV^- identification from NPL (red) and UoM (gray). The NV^- centers examined at NPL are circled. ND#5 represents ND candidate #B, circled in green. b) Power dependence plots of #B measured at UoM (black) and NPL (red). The *vertical* lines correspond to $P_{sat}^{NPL} = 0.39(6)$ mW (solid) and $P_{sat}^{UoM} = 0.089(5)$ mW (dashed), with the full saturation curve (solid), components from the NV^- emission (dashed-dot) and linear residual laser offset (dashed). Note: the x-axes are scaled from 0 to $12P_{sat}$ such that the vertical lines corresponding to P_{sat}^{NPL} and P_{sat}^{UoM} overlap following SPE system calibration. c) $g^{(2)}(t)$ signals for #B with the inset covering a larger coherence window to show bunching decay where $g^{(2)}(t)>1$.

The best 6 potentially single emitters were selected by NPL; these had an RMSE<0.15 and a sufficient SNR to suggest it is a likely SPE with $g^{(2)}(0)<0.5$. These candidates were located at UoM by referencing fiducial markers on the substrate (see Supplement 1). They were examined under the same excitation conditions as NPL as demonstrated in Fig. 1(b), meaning the absorbed fluence was identical, and optoelectronic properties could be compared. In Fig. 2, the three model parameters ($g^{(2)}(0)$, P_{sat}, k_∞) and I_{80} are compared between NPL and UoM, where error bars represent a 1σ uncertainty in the fitting parameter. The $g^{(2)}(0)$ values are expected to be independent from experimental variables, except for laser scatter and detector dark counts. Four NV^- centers were found to have $g^{(2)}(0)<0.5$ (#B, #C, #D, #E) with the remaining 2 having $g^{(2)}(0)>0.5$ (#A, #F). k_∞ is a product of the fundamental emission rate and system throughput, and therefore the ratio of this parameter between NPL and UoM is sensitive to these differences. The ratio of I_{80} between NPL and UoM is also sensitive to variation in the system throughput, as well as the background count rate. Conversely, the target pump power required to reach this count rate depends on the light coupling into the NV^- center, which is primarily sensitive to the excitation beam profile. This is shown by Table 1, where P_{sat} changes between system calibrations.

The uncertainties in Fig. 2 are predominantly attributable to the SNR, which can be improved by acquiring photon streams for a longer duration. However, excitation conditions and polarisation may also play a role. Excitation conditions, such as the wavelength, can affect recombination lifetimes [64] which changes the appearance of the $g^{(2)}(t)$ signal. However, this is not expected to be significant in this work as both systems use nominally identical pump wavelengths. The orientation of the NV^- center dipoles determine the perceived emission rate, by affecting how efficiently the color center is excited by polarised light [65], causing a change in P_{sat}, and the emission profile of the NV^- center. Since the candidates have high emission rates in both NPL and UoM systems, despite sample orientation not being controlled, this indicates that these particular NDs may host favorably oriented emission dipoles resulting in no overall polarisation for absorption or emission where the emission dipoles lay parallel to the focal plane [65]. This

Optics EXPRESS

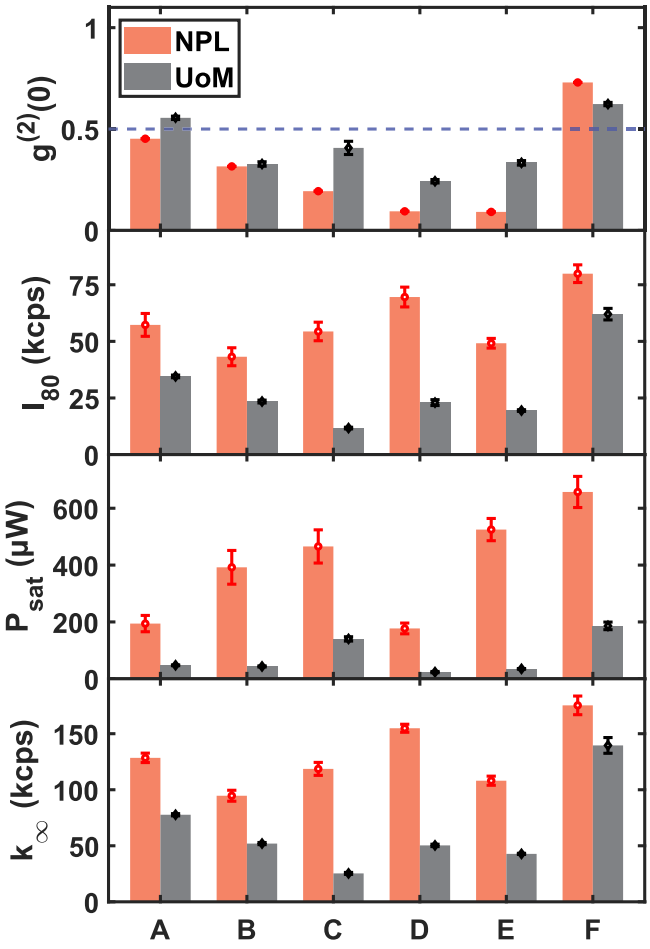

Fig. 2. Parameters of candidate NV^- centers #A-#F correlated between the two systems, NPL (red) and UoM (gray). The blue dashed line represents $g^{(2)}(0) = 0.5$.

is a favourable characteristic for a reference single-photon emitter, as control for polarisation is not required. Therefore while an SPE that emits with $g^{(2)}(0)<0.5$ can be used as an SPE reference, the closer the $g^{(2)}(0)$ value is towards zero, the less variability is expected in emission. Non-single-photon processes such as scattering likely contribute to increased variability in emission rate because, as purely optical effects, they are sensitive to ND orientation and laser pump profile.

Critically, the dissimilarities in throughput reveals a systematic difference in observed properties between laboratories and explains why I_{80}, P_{sat} and k_∞ in Fig. 2 are expected to lie outwith their uncertainty bounds. The pump power density can change with beam alignment between and over the duration of the measurement which is reflected by P_{sat} in Table 1, to reach a k_∞ of 52(1) kcps. This indicates a 3% standard deviation in the determined light throughput at UoM.

The UoM:NPL ratio of I_{80} in Fig. 3 shows that the collection efficiency at UoM is lower than NPL by a ratio of 0.32(7), when only considering single emitters #B, #C, #D and #E. Assuming Lambertian emission, the ratio (UoM:NPL) of light gathering ability solely due to the objective numerical apertures is 0.94, a minor contribution to the overall ratio of I_{80}. Although a multimode fiber was used at UoM, which likely collects more background photons than a single-mode fiber

Optics EXPRESS

at NPL, the photon detection rate at I_{80} was still lower at UoM. Given this approximately 3× reduction in photon detection rate, a 9× increase in acquisition time is required to maintain the same coincidence count. This is reflected in the 3600 s acquisition time for $g^{(2)}(t)$ at UoM, where a ratio of 6× was used that was sufficient for consistent results as shown in Table 1. The 0.2(1) ratio for P_{sat} shows that the excitation efficiency is greater at UoM, with an intrasite standard deviation of 35.8%. Systematic differences between NPL and UoM are shown by the standard deviation of 30.35% in I_{80} and 60.17% in P_{sat}, suggesting that calibration is required for quantitatively comparing inter-site single-photon measurements.

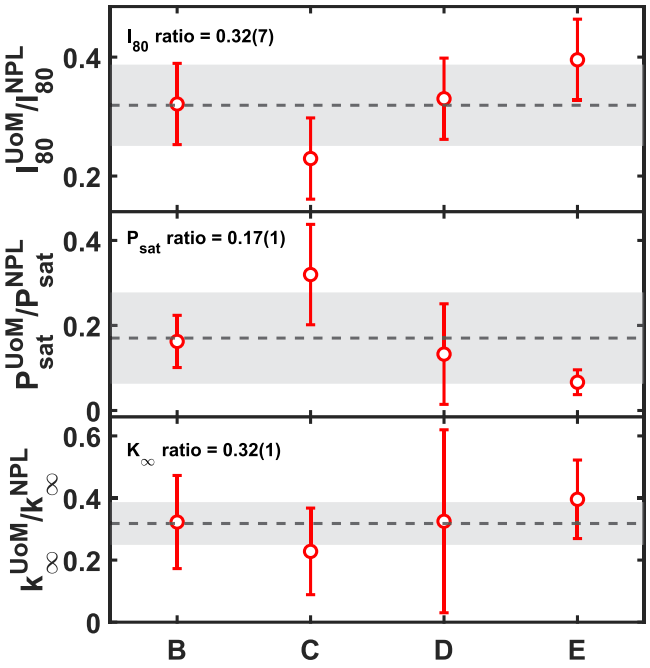

Fig. 3. Ratios of parameters I_{sat}, P_{sat} and k_∞ between NPL and UoM at saturation for single-photon emitting NV^- centers. The error bars represent the $\pm1\sigma$ fitting error for each center, the horizontal dashed black line indicates the mean across these four centers, and shaded regions shows the experimental $\pm1\sigma$ standard deviation across the four centers.

Initial measurements on the 6 candidates showed that emitter #B, shown in Fig. 1(a), was the least sensitive to system alignment, possibly due to favourable orientation of the NV^- center. This candidate gave an I_{80} count rate of 23(1) kcps, as calculated from Table 1, showing a 3% standard deviation upon repeated measurements, which serves as an exemplary SPE for this work. Fig. 1(c) shows that for ND #B the $g^{(2)}(t)$ signal measured at both laboratories are in agreement, with $g^{(2)}_{UoM}(0) = 0.28(7)$ compared to $g^{(2)}_{NPL}(0) = 0.32(3)$. We note that the $g^{(2)}(0)$ of 0.20(1) in Table 1 appears to be an outlier, however, it still confirms that ND #B is an SPE. The sample was repeatedly studied over 3 months (see SI), ND #B was irradiated several times with power densities up to 2.53 MW/cm^2 for up to 3600 s at a time. No optically induced damage was observed. This is compatible with previous studies, which have reported stability that is expected to last for centuries [49], demonstrating the robustness of the NV^- centers hosted in a ND system.

Another color center, #C, did not exhibit any metastable state decay times in its $g^{(2)}(t)$ (see Supplement 1) which is ideal for generation of on-demand single photons [33], as metastable states [55] would otherwise reduce the rate of radiative recombination. This could be due to the local environment of the NV^- centre, where there is an absence of other nitrogen defects in the

Optics EXPRESS

near vicinity that allow a photoinduced electron transfer to enable charge state switching [66]. This would result in a lack of intersystem crossings, and therefore no metastable state decay as the system is prevented from doing so. We note that such NV^- centers are rare, representing less than 0.1% of those studied in the present set.

Although the robust and stable nature of NV^- centers as SPE references has been demonstrated, it is not without caveats. Firstly, it was inefficient to obtain enough candidate reference emitters as only 4 NDs (66.7%) were validated to contain NV^- centers at UoM and only 1 (16.7%) showed repeatable results. The high-throughput data (see Supplement 1) follows a similar trend where 44% of NDs contain single defects [10], yet few are usable as quantum references due to poor signal-to-noise ratio, which is why a subset was selected for remeasurement. An alternative would be to use defect implantation [67–71] for greater specificity over defect concentration, although these techniques are expensive in time and cost. Another approach is to increase the efficiency of the procedure through QR codes etched on the substrate. This would allow machine-assisted location of NDs by automatically calculating the rotation of the sample and routing to the unique code hash closest to the candidate, improving the reliability of location for repeated measurement [72]. Another limitation is that the NV^- centers are most efficiently excited by 510 nm to 575 nm radiation [62,63], confining other measurements to materials that are excited in this wavelength range. It is important to note that the NV centers are sensitive to changes in magnetic field [73], and so this approach is most applicable in the absence of external fields.

4. Conclusion

Since single-photon characterization systems generally differ in both collection and excitation efficiency, robust SPE references are needed for calibration. We have demonstrated that, by measuring the count-rate saturation curves of specific NV^- centers, it is possible to standardize the excitation conditions across different experimental setups, facilitating reliable and repeatable measurements of the single-photon emission rate. The I_{80} count rate ratio of 0.32(7) between UoM:NPL, and the k_∞ ratio of 0.32(1) indicates that this technique can be used to correct for a system's photon throughput. Crucially, when used as a benchmark for other materials, this allows quantitative comparison to externally measured materials using the same technique, with their own NV^- reference. Our cross-site calibration shows that it is possible to use locally identified single NV- centers as a single-photon reference which is portable, stable and robust. This shows promise as a method to standardise comparison of a wide range of quantum materials, supporting work towards realizing deterministic absolute single-photon sources.

Funding. Innovate UK (TS/X002195/1); UK Research and Innovation (MR/T021519/1); Department for Science, Innovation and Technology; Engineering and Physical Sciences Research Council; Leverhulme Trust (ECF-2024-250).

Acknowledgment. We would like to acknowledge Himanshu Shekha and Nu Quantum for provision of registration featured substrates. We thank Dr. Hannah Stern (UoM) for her feedback on an early draft of this work, and Dr. Christopher Chunnilall (NPL) for his useful revisions and contributions to several drafts of this article.

Disclosures. The authors declare no conflicts of interest.

Author Contributions

Nikesh Patel: Methodology (lead), Software (supporting), Validation (equal), Formal Analysis (lead), Investigation (equal), Data curation (lead), Writing - Original Draft (lead), Writing Review & Editing (equal), Visualization (lead).

Benyam Dejen: Methodology (lead), Software (supporting), Validation (equal), Formal Analysis (supporting), Investigation (equal), Data curation (supporting), Writing Review & Editing (equal).

Dr. Stephen Church: Methodology (supporting), Software (lead), Writing - Review & Editing (equal).

Dr. Philip Dolan: Conceptualization (equal), Methodology (lead), Software (lead), Validation (equal), Formal analysis (supporting), Resources (lead), Writing - Review & Editing (equal), Supervision (equal), Project administration (equal), Funding acquisition (equal).

Dr. Patrick Parkinson: Conceptualization (equal), Methodology (lead), Software (lead), Validation (equal), Formal analysis (supporting), Resources (lead), Writing - Review & Editing (equal), Visualization (supporting), Supervision (equal), Project administration (equal), Funding acquisition (equal).

Optics EXPRESS

Data availability. The data that support the findings of this study are openly available in Figshare at [74]. The code associated with the analysis is available at [75].

Supplemental document. See Supplement 1 for supporting content.

References

1. D. Terada, T. F. Segawa, A. I. Shames, *et al.*, "Monodisperse Five-Nanometer-Sized Detonation Nanodiamonds Enriched in Nitrogen-Vacancy Centers," ACS Nano **13**(6), 6461–6468 (2019).
2. X. Li, S. Liu, Y. Wei, *et al.*, "Bright semiconductor single-photon sources pumped by heterogeneously integrated micropillar lasers with electrical injections," Light:Sci. Appl. **12**(1), 65 (2023).
3. C. M. Valensise, I. Grecco, D. Pierangeli, *et al.*, "Large-scale photonic natural language processing," Photonics Res. **10**(12), 2846 (2022).
4. X. Liu, K. Akahane, N. A. Jahan, *et al.*, "Single-photon emission in telecommunication band from an InAs quantum dot grown on InP with molecular-beam epitaxy," Appl. Phys. Lett. **103**(6), 061114 (2013).
5. F. B. Basset, M. Valeri, E. Roccia, *et al.*, "Quantum key distribution with entangled photons generated on demand by a quantum dot," Sci. Adv. **7**(12), 6379 (2021).
6. M. E. Bathen and L. Vines, "Manipulating Single-Photon Emission from Point Defects in Diamond and Silicon Carbide," Adv. Quantum Technol. **4**(7), 2100003 (2021).
7. L. Zhai, G. N. Nguyen, C. Spinnler, *et al.*, "Quantum interference of identical photons from remote GaAs quantum dots," Nat. Nanotechnol. **17**(8), 829–833 (2022).
8. A. M. Day, J. R. Dietz, M. Sutula, *et al.*, "Laser writing of spin defects in nanophotonic cavities," Nat. Mater. **22**(6), 696–702 (2023).
9. L. Li, L. D. Santis, I. B. W. Harris, *et al.*, "Heterogeneous integration of spin–photon interfaces with a CMOS platform," Nature **630**(8015), 70–76 (2024).
10. B. D. Wood, G. A. Stimpson, J. E. March, *et al.*, "Long spin coherence times of nitrogen vacancy centers in milled nanodiamonds," Phys. Rev. B **105**(20), 205401 (2022).
11. A. H. Proppe, D. B. Berkinsky, H. Zhu, *et al.*, "Highly stable and pure single-photon emission with 250 ps optical coherence times in InP colloidal quantum dots," Nat. Nanotechnol. **18**(9), 993–999 (2023).
12. S.-W. Feng, C.-Y. Cheng, C.-Y. Wei, *et al.*, "Purification of Single Photons from Room-Temperature Quantum Dots," Phys. Rev. Lett. **119**(14), 143601 (2017).
13. M. E. Reimer, G. Bulgarini, N. Akopian, *et al.*, "Bright single-photon sources in bottom-up tailored nanowires," Nat. Commun. **3**(1), 737 (2012).
14. M. T. Borgström, V. Zwiller, E. Müller, *et al.*, "Optically bright quantum dots in single nanowires," Nano Lett. **5**(7), 1439–1443 (2005).
15. M. Heiss, Y. Fontana, A. Gustafsson, *et al.*, "Self-assembled quantum dots in a nanowire system for quantum photonics," Nat. Mater. **12**(5), 439–444 (2013).
16. S. Lazić, A. Hernández-Mínguez, and P. V. Santos, "Control of single photon emitters in semiconductor nanowires by surface acoustic waves," Semicond. Sci. Technol. **32**(8), 084002 (2017).
17. B. Loitsch, J. Winnerl, G. Grimaldi, *et al.*, "Crystal Phase Quantum Dots in the Ultrathin Core of GaAs-AlGaAs Core-Shell Nanowires," Nano Lett. **15**(11), 7544–7551 (2015).
18. D. Nelson, S. Byun, J. Bullock, *et al.*, "Colloidal quantum dots as single photon sources," J. Mater. Chem. C **12**(16), 5684–5695 (2024).
19. B. Wang, J. W. M. Lim, S. M. Loh, *et al.*, "Weakly confined organic–inorganic halide perovskite quantum dots as high-purity room-temperature single photon sources," ACS Nano **18**(16), 10807–10817 (2024).
20. J. Wang, L. He, Y. Zhang, *et al.*, "Locally strained 2d materials: Preparation, properties, and applications," Adv. Mater. **36**(23), 2314145 (2024).
21. S. Chen, C. Wang, H. Cai, *et al.*, "Realization of single-photon emitters with high brightness and high stability and excellent monochromaticity," Matter **7**(3), 1106–1116 (2024).
22. X. Chen, X. Yue, L. Zhang, *et al.*, "Activated single photon emitters and enhanced deep-level emissions in hexagonal boron nitride strain crystal," Adv. Funct. Mater. **34**(1), 2306128 (2024).
23. C. Haws, E. Perez, M. Davanco, *et al.*, "Broadband, efficient extraction of quantum light by a photonic device comprised of a metallic nano-ring and a gold back reflector," Appl. Phys. Lett. **120**(8), 81103 (2022).
24. S. Adekanye, H.-C. Chang, D. Hunger, *et al.*, "Robust, tunable, and high purity triggered single photon source at room temperature using a nitrogen-vacancy defect in diamond in an open microcavity," Opt. Express **26**(6), 7056–7065 (2018).
25. V. Giovannetti, S. Lloyd, L. Maccone, *et al.*, "Quantum-enhanced measurements: Beating the standard quantum limit," Phys. Rev. Lett. **68**(2), 135–138 (1992).
26. P. P. Iyer, S. Prescott, S. Addamane, *et al.*, "Control of Quantized Spontaneous Emission from Single GaAs Quantum Dots Embedded in Huygens' Metasurfaces," Nano Lett. **24**, 4749–4757 (2024).
27. M. Esmann, S. C. Wein, and C. Antón-Solanas, "Solid-state single-photon sources: Recent advances for novel quantum materials," Adv. Funct. Mater. **34**(30), 2315936 (2024).
28. R. J. Glauber, "The Quantum Theory of Optical Coherence," Phys. Rev. **130**(6), 2529–2539 (1963).
29. D. Bluvstein, Z. Zhang, and A. C. Jayich, "Identifying and Mitigating Charge Instabilities in Shallow Diamond Nitrogen-Vacancy Centers," Phys. Rev. Lett. **122**(7), 076101 (2019).

Optics EXPRESS

30. M. W. Doherty, N. B. Manson, P. Delaney, *et al.*, "The nitrogen-vacancy colour centre in diamond," Phys. Rep. **528**(1), 1–45 (2013).
31. B. Rodiek, M. Lopez, H. Hofer, *et al.*, "Experimental realization of an absolute single-photon source based on a single nitrogen vacancy center in a nanodiamond," Optica **4**(1), 71 (2017).
32. B. Lounis and M. Orrit, "Single-photon sources," Rep. Prog. Phys. **68**(5), 1129–1179 (2005).
33. M. D. Eisaman, J. Fan, A. Migdall, *et al.*, "Single-photon sources and detectors," Rev. Sci. Instrum. **82**(7), 71101 (2011).
34. R. Brouri, A. Beveratos, J.-P. Poizat, *et al.*, "Photon antibunching in the fluorescence of individual color centers in diamond," Opt. Lett. **25**(17), 1294 (2000).
35. C. Kurtsiefer, S. Mayer, P. Zarda, *et al.*, "Stable Solid-State Source of Single Photons," Phys. Rev. Lett. **85**(2), 290–293 (2000).
36. J. Botsoa, T. Sauvage, M.-P. Adam, *et al.*, "Optimal conditions for NV-center formation in type-1b diamond studied using photoluminescence and positron annihilation spectroscopies," Phys. Rev. B **84**(12), 125209 (2011).
37. G. Dantelle, A. Slablab, L. Rondin, *et al.*, "Efficient production of NV colour centres in nanodiamonds using high-energy electron irradiation," J. Lumin. **130**(9), 1655–1658 (2010).
38. A. Beveratos, S. Kühn, R. Brouri, *et al.*, "Room temperature stable single-photon source," Eur. Phys. J. D **18**(2), 191–196 (2002).
39. E. M. Purcell, H. C. Torrey, and R. V. Pound, "Resonance Absorption by Nuclear Magnetic Moments in a Solid," Phys. Rev. **69**(1-2), 37–38 (1946).
40. A. S. Zalogina, R. S. Savelev, E. V. Ushakova, *et al.*, "Purcell effect in active diamond nanoantennas," Nanoscale **10**(18), 8721–8727 (2018).
41. A. Krueger and D. Lang, "Functionality is Key: Recent Progress in the Surface Modification of Nanodiamond," Adv. Funct. Mater. **22**(5), 890–906 (2012).
42. F. Hirt, J. Christinck, H. Hofer, *et al.*, "Sample fabrication and metrological characterization of single-photon emitters based on nitrogen vacancy centers in nanodiamonds," Eng. Res. Express **3**(4), 045038 (2021).
43. I. Cardoso Barbosa, J. Gutsche, D. Lönard, *et al.*, "Temperature dependence of charge conversion during nv-center relaxometry in nanodiamond," Phys. Rev. Res. **6**(2), 023078 (2024).
44. S. Kück, M. López, H. Hofer, *et al.*, "Single photon sources for quantum radiometry: a brief review about the current state-of-the-art," Appl. Phys. B **128**(2), 28 (2022).
45. M. von Helversen, J. Böhm, M. Schmidt, *et al.*, "Quantum metrology of solid-state single-photon sources using photon-number-resolving detectors," New J. Phys. **21**(3), 035007 (2019).
46. E. Moreva, P. Traina, R. A. Kirkwood, *et al.*, "Feasibility study towards comparison of the g(2)(0) measurement in the visible range," Metrologia **56**(1), 015016 (2019).
47. F. Jelezko and J. Wrachtrup, "Single defect centres in diamond: A review," Phys. Status Solidi A **203**, 3207–3225 (2006).
48. H.-S. Jung and K. C. Neuman, "Surface modification of fluorescent nanodiamonds for biological applications," Nanomaterials **11**(1), 153 (2021).
49. C. Laube, R. Temme, A. Prager, *et al.*, "Fluorescence lifetime control of nitrogen vacancy centers in nanodiamonds for long-term information storage," ACS Nano **17**(16), 15401–15410 (2023).
50. Y.-R. Chang, H.-Y. Lee, K. Chen, *et al.*, "Mass production and dynamic imaging of fluorescent nanodiamonds," Nat. Nanotechnol. **3**(5), 284–288 (2008).
51. S.-J. Yu, M.-W. Kang, H.-C. Chang, *et al.*, "Bright fluorescent nanodiamonds:? no photobleaching and low cytotoxicity," J. Am. Chem. Soc. **127**(50), 17604–17605 (2005).
52. P. Reineck, D. W. M. Lau, E. R. Wilson, *et al.*, "Effect of surface chemistry on the fluorescence of detonation nanodiamonds," ACS Nano **11**(11), 10924–10934 (2017).
53. M. Berthel, O. Mollet, G. Dantelle, *et al.*, "Photophysics of single nitrogen-vacancy centers in diamond nanocrystals," Phys. Rev. B **91**(3), 035308 (2015).
54. C. Laube, T. Oeckinghaus, J. Lehnert, *et al.*, "Controlling the fluorescence properties of nitrogen vacancy centers in nanodiamonds," Nanoscale **11**(4), 1770–1783 (2019).
55. X. Li, J. Storteboom, S. Castelletto, *et al.*, "Lifetime investigation of single nitrogen vacancy centres in nanodiamonds," Opt. Express **23**(9), 11327–11333 (2015).
56. G. Waldherr, J. Beck, M. Steiner, *et al.*, "Dark States of Single Nitrogen-Vacancy Centers in Diamond Unraveled by Single Shot NMR," Phys. Rev. Lett. **106**(15), 157601 (2011).
57. M. V. Hauf, B. Grotz, B. Naydenov, *et al.*, "Chemical control of the charge state of nitrogen-vacancy centers in diamond," Phys. Rev. B **83**(8), 081304 (2011).
58. K. Y. Han, S. K. Kim, C. Eggeling, *et al.*, "Metastable dark states enable ground state depletion microscopy of nitrogen vacancy centers in diamond with diffraction-unlimited resolution," Nano Lett. **10**(8), 3199–3203 (2010).
59. H. R. Brown and R. Q. Twiss, "Correlation between Photons in two Coherent Beams of Light," Nature **177**(4497), 27–29 (1956).
60. S. Kumar, S. K. Andersen, and S. I. Bozhevolnyi, "Coupling of nitrogen-vacancy centers in a nanodiamond to a silver nanocube," Opt. Mater. Express **6**(1), 29–3406 (2016).
61. A. Dräbenstedt, L. Fleury, C. Tietz, *et al.*, "Low-temperature microscopy and spectroscopy on single defect centers in diamond," Phys. Rev. B **60**(16), 11503–11508 (1999).

Optics EXPRESS

62. K. Beha, A. Batalov, N. B. Manson, *et al.*, "Optimum Photoluminescence Excitation and Recharging Cycle of Single Nitrogen-Vacancy Centers in Ultrapure Diamond," Phys. Rev. Lett. **109**(9), 097404 (2012).
63. N. Aslam, G. Waldherr, P. Neumann, *et al.*, "Photo-induced ionization dynamics of the nitrogen vacancy defect in diamond investigated by single-shot charge state detection," New J. Phys. **15**(1), 013064 (2013).
64. P. Ji, R. Balili, J. Beaumariage, *et al.*, "Multiple-photon excitation of nitrogen vacancy centers in diamond," Phys. Rev. B **97**(13), 134112 (2018).
65. P. R. Dolan, X. Li, J. Storteboom, *et al.*, "Complete determination of the orientation of NV centers with radially polarized beams," Opt. Express **22**(4), 4379 (2014).
66. T. Gaebel, M. Domhan, C. Wittmann, *et al.*, "Photochromism in single nitrogen-vacancy defect in diamond," Appl. Phys. B **82**(2), 243–246 (2006).
67. M. Adshead, M. Coke, G. Aresta, *et al.*, "A High-Resolution Versatile Focused Ion Implantation Platform for Nanoscale Engineering," Adv. Eng. Mater. **25**(22), 2300889 (2023).
68. J. R. Rabeau, P. Reichart, G. Tamanyan, *et al.*, "Implantation of labelled single nitrogen vacancy centers in diamond using 15N," Appl. Phys. Lett. **88**(2), 1–3 (2006).
69. J. O. Orwa, C. Santori, K. M. C. Fu, *et al.*, "Engineering of nitrogen-vacancy color centers in high purity diamond by ion implantation and annealing," J. Appl. Phys. **109**(8), 083530 (2011).
70. Y. Chu, N. de Leon, B. Shields, *et al.*, "Coherent Optical Transitions in Implanted Nitrogen Vacancy Centers," Nano Lett. **14**(4), 1982–1986 (2014).
71. J. Meijer, B. Burchard, M. Domhan, *et al.*, "Generation of single color centers by focused nitrogen implantation," Appl. Phys. Lett. **87**(26), 1–3 (2005).
72. M. Sutula, I. Christen, E. Bersin, *et al.*, "Large-scale optical characterization of solid-state quantum emitters," Nat. Mater. **22**(11), 1338–1344 (2023).
73. A. Gruber, A. Dräbenstedt, C. Tietz, *et al.*, "Scanning confocal optical microscopy and magnetic resonance on single defect centers," Science **276**(5321), 2012–2014 (1997).
74. P. Nikesh, B. Dejen, P. Dolan, *et al.*, "Research data for 'nitrogen-vacancy color centers in nanodiamonds as reference single-photon emitters'," figshare v1 (2024), https://figshare.manchester.ac.uk/articles/dataset/Research_Data_for_Nitrogen-Vacancy_Color_Centers_in_Nanodiamonds_as_Reference_Single-Photon_Emitters_/27290712
75. P. Nikesh, B. Dejen, P. Dolan, *et al.*, "OMS-lab/nanodiamond-nitrogen-vacancy-reference-emitters," Github, (2024), [accessed date 05/30/2025], https://github.com/OMS-lab/Nanodiamond-Nitrogen-Vacancy-Reference-Emitters.